Journal of Solid State Chemistry **160,** 350–352 (2001)
doi:10.1006/jssc.2001.9239, available online at http://www.idealibrary.com on IDEAL®

Phonon Modes of $A(Co_{1/2}Mn_{1/2})$ O_3 (A = La, Nd, Dy, Ho, Yb)

F. Gao, R. A. Lewis, X. L. Wang, and S. X. Dou

Institute for Superconducting and Electronic Materials, University of Wollongong, Wollongong 2522, Australia

Received January 3, 2001; in revised form April 26, 2001; accepted May 11, 2001; published online July 26, 2001

Phonon energies in cobaltite/manganites $A(Co_{1/2}Mn_{1/2})O_3$, where A is a lanthanide, have been determined by far-infrared spectroscopy. The phonon energies systematically shift and split and new modes appear as the mass of the lanthanide is increased through the series A = La, Nd, Dy, Ho, Yb. The behavior of the phonon modes correlates with the magnetic properties of this series of compounds, in particular with the appearance of metamagnetism for the compounds with smaller ions on the A site.

I. INTRODUCTION

Perovskites have the formula ABX_3. In this work we deal with perovskites in which A is a rare-earth element, B is cobalt or manganese with equal likelihood, and X is oxygen. In contrast to the ideal perovskite structure, which is cubic, such ternary oxides are found to be orthorhombic. As the radius of the rare-earth ion on the A site decreases, the distortion of the lattice away from cubicity increases and the unit cell volume decreases. At the B site the Co or Mn ion resides at the center of an O octahedron. The Co/Mn ions order in a NaCl structure, as verified by superlattice lines being observed in X-ray diffraction patterns (1). The fraction of misplaced Co/Mn ions is estimated to be 7.5% (2). NMR data support this structure (3, 4).

The cobaltite/manganite perovskites $A(Co_{1/2}Mn_{1/2})$ O_3, where A is a lanthanide, exhibit ferromagnetism. The ferromagnetism arises from the superexchange interaction between Co^{2+} and Mn^{4+} ions mediated by O^{2-} (2). The Curie temperature, T_C, is relatively high and decreases systematically with decreasing radius of the ion on the A site (1). The Co^{2+}–O^{2-}–Mn^{4+} superexchange is maximized when the Co–O–Mn angle is a straight angle, corresponding to the ideal perovskite cubic structure. The magnetic behavior of rare-earth cobaltite/manganite perovskites is therefore seen to be intimately related to their structure.

Troyanchuk *et al.* (1) distinguish between the magnetic behavior of $A(Co_{1/2}Mn_{1/2})O_3$ compounds having larger ions (La, Pr, Nd, Sm, Eu) and those having smaller ions (Gd, Tb, Dy, Y, Ho) on the A site. The temperature dependence of the magnetization of the latter, field cooled in fields above 400 kOe, exhibits a sharp peak in magnetization around T_C; the temperature dependence of the magnetization of the former does not. The field dependence of the magnetization of the latter exhibits a sharp increase at a critical field H_C and a large magnetic hysteresis; that of the former does not. Troyanchuk *et al.* (1) conclude that the compounds containing smaller rare-earth ions are metamagnets. The metamagnetism is attributed to competition between magnetic anisotropy and the superexchange interaction in an applied magnetic field.

II. EXPERIMENTAL

Ceramic samples were prepared by conventional sintering. After mixing the starting materials, sintering was carried out at 1100°C. The sintered material was then ground and sintered again at 1150°C. The preparation, structure, and magnetic properties have been described in detail elsewhere for $Gd(Co_{1/2}Mn_{1/2})O_3$ (5) and $Yb(Co_{1/2}Mn_{1/2})O_3$ (6).

Samples were prepared for reflectivity measurements by crushing the resintered material and compacting it into pellets. The pellets were then polished to 1 μm. Reflectivity was measured at near-normal incidence at room temperature using a Bomem DA3.26 rapid-scan interferometer equipped with a DTGS detector. A polished brass block was used as a reflection reference.

To prepare samples for transmission measurements, the resintered material was crushed and diluted with CsI. Pellets were then prepared. Optimum spectra were obtained using ~0.45 g of material dispersed in 100 g of carrier. The method of preparation has been previously applied to lanthanum manganites (7). The transmission measurements employed the same spectrometer and detector as the reflectivity measurements.

III. RESULTS AND DISCUSSION

Reflectivity spectra were found to be similar for doping with different lanthanides. Figure 1 gives data for A = Dy, which lies in the middle of the range of lanthanides

0022-4596/01 $35.00

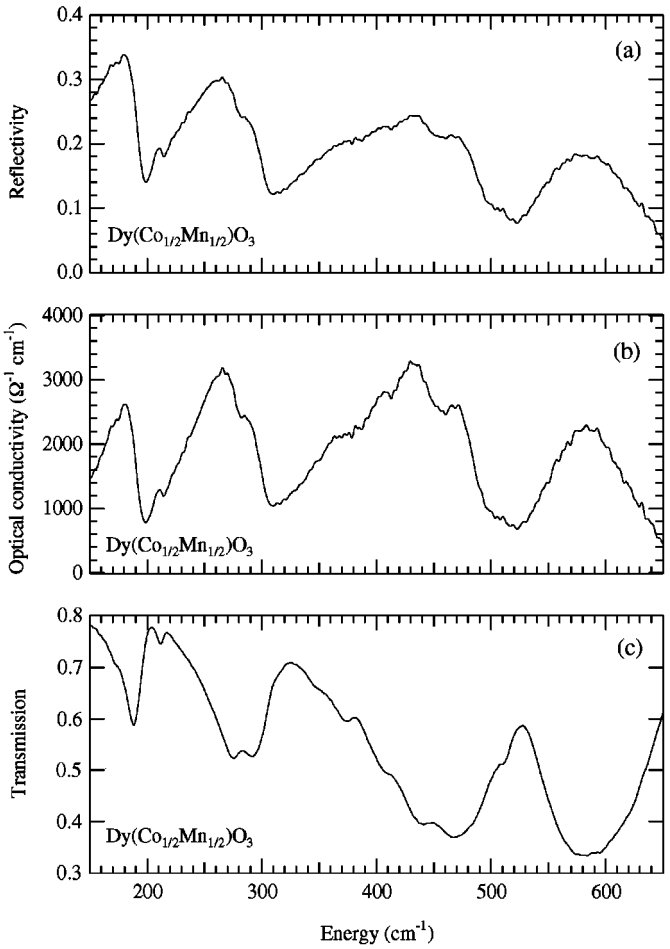

FIG. 1. Far-infrared spectra of $Dy(Co_{1/2}Mn_{1/2})O_3$. (a) Absolute reflectivity at near-normal incidence. (b) Optical conductivity calculated from (a) using Kramers–Kronig transformation. (c) Transmission of powder.

investigated. The top panel (Fig. 1a) gives the absolute reflectivity. The middle panel (Fig. 1b) gives the optical conductivity, derived from the reflectivity spectrum through a Kramers– Kronig transformation. The bottom panel (Fig. 1c) gives the transmission spectrum.

The optical modes of the ideal cubic perovskite structure have irreducible representation $\Gamma = 3F_{1u}$ (infrared active) $+ F_{2u}$ (infrared inactive). Thus three threefold degenerate infrared active modes are expected for wave vector $\mathbf{k} = 0$. Last (8) identifies the bands in order of increasing energy as an external A–(BX_3) vibration, X–B–X bending, and B–X stretching. As the crystal symmetry is reduced, more optical modes are expected. There are 25 infrared active modes for orthorhombic (D_{2h}^{16}, *Pnma*) symmetry (9). In particular, the forbidden torsional mode F_{2u} (O_h^1) is now allowed and has been calculated to lie between the external and bending mode (10). Consequently, the four broad bands in Fig. 1c at $\omega_1 \sim 200\ cm^{-1}$, $\omega_2 \sim 300\ cm^{-1}$, $\omega_3 \sim 400\ cm^{-1}$, and $\omega_4 \sim 600\ cm^{-1}$ are assigned to external, torsional, bending, and stretching modes, respectively.

In view of little difference being noted in the reflectivity spectra for doping with different lanthanides, we will henceforth concentrate on the transmission spectra. Transmission spectra for $A(Co_{1/2}Mn_{1/2})O_3$ (A = La, Nd, Dy, Ho, Yb) are displayed in Fig. 2. The behavior of the four main bands is as follows. The external vibration ($\sim 200\ cm^{-1}$) increases in energy then decreases. The maximum energy of this band, of the materials studied, occurs for A = Dy. The torsional band ($\sim 300\ cm^{-1}$) splits, with the splitting first increasing down the lanthanide series, then decreasing again. Of the materials studied, the greatest splitting occurs for A = Dy. The bending band ($\sim 400\ cm^{-1}$) shows the most dramatic behavior. The center of mass shifts systematically to higher energy. The band originally appears split in two. As the atomic number of the lanthanide increases, up to four components become evident. The stretching band

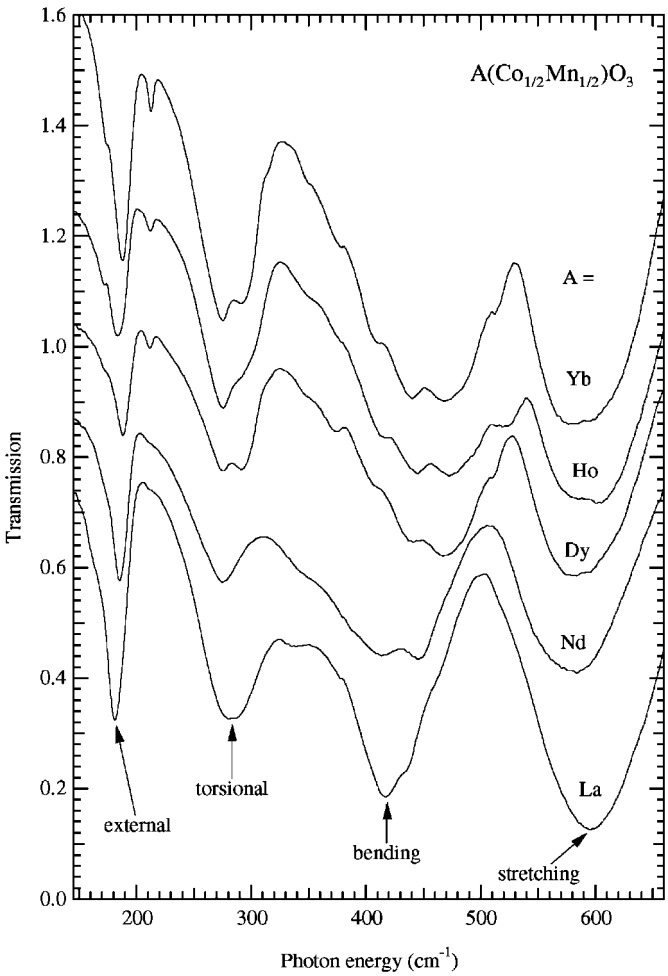

FIG. 2. Far-infrared spectra of $A(Co_{1/2}Mn_{1/2})O_3$ for A = La (bottom), Nd, Dy, Ho, Yb (top). Successive spectra have been offset for clarity.

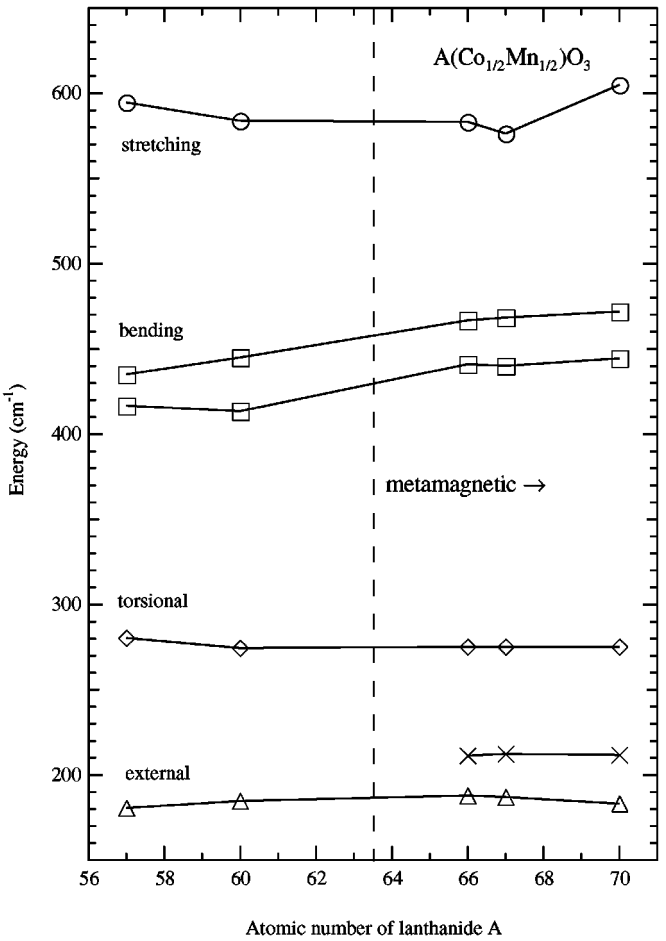

FIG. 3. Variation in energy of principal phonon bands in $A(Co_{1/2}Mn_{1/2})O_3$ with the atomic number of the ion on the A site.

($\sim 600\ cm^{-1}$) both splits, with the separation of the components increasing with atomic number of the lanthanide, and shifts first to lower, then to higher energy. Other, weaker bands are seen to develop on either side of the external band ($\sim 180\ cm^{-1}$, $\sim 210\ cm^{-1}$) and around $\sim 380\ cm^{-1}$.

The energies of the main phonon modes are presented as a function of lanthanide atomic number in Fig. 3. As noted in the Introduction, metamagnetism has been observed in these compounds if the atomic number of the lanthanide is 64 or more. There is a clear correlation between this magnetic behavior and the phonon modes as summarized in Fig. 3. The external mode at first increases in energy with decreasing ionic radius at the A site, which is consistent with increasing distortion, reaching a maximum near the metamagnetic crossover. At this point the smaller bands on either side ($\sim 180\ cm^{-1}$, $\sim 210\ cm^{-1}$) become prominent, presumably as a result of further lowering of symmetry. The appearance of the subsidiary band at higher energy ($\sim 210\ cm^{-1}$) accounts for the decreasing energy of the main external band as the atomic mass of the lanthanide increases beyond the metamagnetic crossover. The dependence of the bending and stretching modes, related respectively to the distance B–X and the angle B–X–B, on the radius of the ion on the A site, and the effect on the infrared spectrum have been discussed by Arulraj and Rao (11) in the context of the compounds $Ln_{1/2}A_{1/2}MnO_3$. As the radius of the ion on the A site decreases, the distance B–X increases while the angle B–X–B decreases. Increasing the distance B–X should decrease the energy of the stretching mode. This is what is observed (Fig. 3), until the crossover to metamagnetism, after which the stretching mode energy increases again. Decreasing the angle B–X–B should increase the energy of the bending mode. As may be seen from Fig. 3, the predicted increase in bending mode energy occurs across the whole range of ionic radii. The sensitivity of the bending mode to A site species has previously been noted for Ca substituting for La in $LaMnO_3$ (12). The bending mode both broadened and shifted to higher energy as the Ca content increased. The same dependence of the bending mode on A site substitution is observed here for $A(Co_{1/2}Mn_{1/2})O_3$.

IV. CONCLUSION

We report the far-infrared spectra for lanthanide cobaltite/manganite perovskites $A(Co_{1/2}Mn_{1/2})O_3$ (A = La, Nd, Dy, Ho, Yb). The spectra show broadly similar features, but splitting and shifts in the phonon energies occur as the radius of the lanthanide species is decreased. The data suggest a strong correlation between the phonon modes and the magnetic properties of these compounds, most likely through the electron–phonon interaction.

ACKNOWLEDGMENTS

The work was supported in part by the Australian Research Council and the University of Wollongong.

REFERENCES

1. I. O. Troyanchuk, N. V. Samsonenko, E. F. Shapovalova, H. Szymczak, and A. Nabialek, *Mater. Res. Bull.* **32,** 67 (1997).
2. G. Blasse, *J. Phys. Chem. Solids* **26,** 1969 (1965).
3. M. Sonobe and K. Asai, *J. Phys. Soc. Japan* **61,** 4193 (1992).
4. N. Nishimori, K. Asai, and M. Mizoguchi, *J. Phys. Soc. Japan* **64,** 1326 (1995).
5. X. L. Wang, *Solid State Commun.*, in press (2001).
6. X. L. Wang, in preparation (2001).
7. F. Gao, R. A. Lewis, X. L. Wang, and S. X. Dou, *Physica C*: *Superconductivity* **341–348,** 2235 (2000).
8. J. T. Last, *Phys. Rev.* **105,** 1740 (1957).
9. Q. Williams, R. Jeanloz, and P. McMillan, *J. Geophys. Res.* **27,** 8116 (1987).
10. I. Nakagawa, A. Tsuchida, and T. Shimanouchi, *J. Chem. Phys.* **47,** 982 (1967).
11. A. Arulraj and C. N. R. Rao, *J. Solid State Chem.* **145,** 557 (1999).
12. S. Faaland, K. D. Knudsen, M.-A. Einarsrud, L. Rørmark, R. Høier, and T. Grande, *J. Solid State Chem.* **140,** 557 (1998).